

Reducing rejection exponentially improves Markov chain Monte Carlo sampling

Hidemaro Suwa^{1,*}

¹*Department of Physics, The University of Tokyo, Tokyo 113-0033, Japan*
(Dated: August 9, 2022)

The choice of the transition kernel essentially determines the performance of the Markov chain Monte Carlo method. Despite the importance of kernel choice, guiding principles for optimal kernels have not been established. We here propose a rejection-controlling one-parameter transition kernel that can be applied to various Monte Carlo samplings and demonstrate that the rejection process plays a major role in determining the sampling efficiency. Varying the rejection probability, we study the autocorrelation time of the order parameter in the two- and three-dimensional ferromagnetic Potts models at the transition temperature. As the rejection rate is reduced, the autocorrelation time decreases exponentially in the sequential spin update and algebraically in the random spin update. The autocorrelation times of conventional algorithms almost fall on a single curve as a function of the rejection rate. The present transition kernel with an optimal parameter provides one of the most efficient samplers for general cases of discrete variables.

I. INTRODUCTION

The choice of the transition kernel, or the transition probability, is essential in the Markov chain Monte Carlo (MCMC) method [1, 2]. A well-chosen transition kernel accelerates distribution convergence and reduces autocorrelation significantly. The transition kernel keeps the global balance, which guarantees the invariance of a target distribution from which states are sampled. The global balance is not a tight condition, leaving much room for optimization. In many applications, the detailed balance, or the reversibility, is additionally imposed as a sufficient condition for the global balance. Although detailed balance is not necessary for sampling from a stationary distribution [3], it becomes easy to set an appropriate transition kernel thanks to the reversibility. A number of reversible samplers have been proposed, such as the Metropolis algorithm [4], the heat bath algorithm [5, 6], the Metropolized Gibbs sampler [7], and the iterative Metropolized Gibbs sampler [8]. Recently, several nonreversible samplers have been developed to achieve faster convergence and smaller statistical errors, such as the Suwa-Todo algorithm [9], lifting techniques [10–14], and the event-chain Monte Carlo method [15, 16]. Nevertheless, guiding principles for optimal transition kernels have not been established. For a finite state space spanned by discrete variables, the autocorrelation time can be represented by the eigenvalues of the transition matrix [8, 17]. The optimization problem of the transition matrix is equivalent to controlling eigenvalues by tuning matrix elements, which is highly non-trivial for a huge matrix typical in statistical mechanical problems.

It has been shown that rejection minimization algorithms outperform the Metropolis and the heat bath algorithms in several models [9, 18, 19]. Because it should be favorable to allow exploring the state space quickly in the

MCMC update, the rejection process, leaving the configuration unchanged, naturally deteriorates the sampling efficiency. It is mathematically proved that a reversible transition matrix with larger off-diagonal elements produces a smaller asymptotic variance, that is, a higher sampling efficiency [17]. This mathematical theorem implies that decreasing diagonal elements, namely rejection probabilities, provides a better sampler. However, this theorem does not apply to nonreversible cases. Detailed studies on the relation between the rejection rate and the sampling efficiency are lacking. It is thus desirable to develop an approach to controlling the rejection probability and perform a systematic study on the effect of the rejection process.

In the present paper, we propose a one-parameter transition kernel that controls the rejection probability in the MCMC method. The single parameter determines the shift of the cumulative distribution of the configuration weights. The present algorithm always holds the global balance and additionally ensures the detailed balance with a particular parameter choice. We can easily find optimal parameters to minimize the rejection probability. Reviewing the optimization problem and previous approaches in Sec. II, we present our approach in a graphical picture and an analytical expression in Sec. III. The rejection effect on the sampling efficiency is investigated for the square and the simple cubic lattice ferromagnetic Potts models at the transition temperature in Sec. IV. As the rejection probability is reduced, the sampling efficiency improves exponentially in the sequential spin update and algebraically in the random spin update. The autocorrelation times of the reference algorithms almost collapse onto a single curve as a function of the rejection rate, indicating that the rejection process is a major factor in determining the sampling efficiency of the MCMC method. The present paper is concluded in Sec. V.

* suwaro@phys.s.u-tokyo.ac.jp

II. PROBABILITY OPTIMIZATION

We here briefly review the optimization problem of the transition kernel and previous approaches. Let us consider a finite state space S spanned by discrete state variables and a Monte Carlo sampling from a target distribution $\pi : S \rightarrow \mathbb{R}$. Our task is to optimize the transition kernel, or the transition matrix P , under the condition of the distribution invariance, namely the global balance [3]:

$$\pi_i = \sum_{j \in S} P_{ij} \pi_j \quad \forall i \in S, \quad (1)$$

where π_i is the weight, or the measure, of state $i \in S$, P_{ij} is the transition probability from j to i , and $\sum_i P_{ij} = 1$. If a transition matrix satisfies the detailed balance condition

$$P_{ij} \pi_j = P_{ji} \pi_i \quad \forall i, j \in S, \quad (2)$$

it is called reversible with respect to π . Detailed balance is sufficient for global balance but not necessary.

In the MCMC method, one needs to reduce autocorrelation between samples. The autocorrelation function [1, 2] of an estimator \hat{O} is defined by

$$A_{\hat{O}}(t) = \frac{\langle \mathcal{O}_{i+t} \mathcal{O}_i \rangle - \langle \hat{O} \rangle^2}{\langle \hat{O}^2 \rangle - \langle \hat{O} \rangle^2}, \quad (3)$$

where \mathcal{O}_t is the sample of the estimator at the t th Monte Carlo step, and $\langle \cdot \rangle$ denotes the Monte Carlo average. This function (3) becomes almost independent of i after the thermalization, or the burn-in. In many cases, the autocorrelation function decays exponentially for large t : $A_{\hat{O}}(t) \sim e^{-t/\tau_{\text{exp}, \hat{O}}}$, where $\tau_{\text{exp}, \hat{O}}$ is the exponential autocorrelation time, given by the second largest eigenvalue of the transition matrix. The sampling efficiency of the MCMC method can be quantified by the integrated autocorrelation time:

$$\tau_{\text{int}, \hat{O}} = \frac{1}{2} + \sum_{t=1}^{\infty} A_{\hat{O}}(t). \quad (4)$$

For reversible cases, it is straightforward to obtain the relation between the integrated autocorrelation time and the eigenvalues of the transition matrix [8, 17]. Thus, the optimization problem of the transition kernel is equivalent to controlling the eigenvalues of a transition matrix by tuning matrix elements [20, 21], which is highly non-trivial for a vast matrix.

Fortunately, Peskun's theorem [17] provides a practical route to improving reversible Markov chains. Let us define an order of matrices: $P_2 \geq P_1$ for any two transition matrices if each of the off-diagonal elements of P_2 is greater than or equal to the corresponding off-diagonal elements of P_1 . The following is Theorem 2.1.1 of Ref. [17].

Theorem 1 (Peskun) *Suppose each of the irreducible transition matrices P_1 and P_2 is reversible for a same*

invariant probability distribution π . If $P_2 \geq P_1$, then, for any f ,

$$v(f, P_1, \pi) \geq v(f, P_2, \pi), \quad (5)$$

where

$$v(f, P, \pi) = \lim_{M \rightarrow \infty} M \text{Var}(\hat{I}_M), \quad (6)$$

and $\hat{I}_M = \sum_{i=1}^M f(x_i)/M$ is an estimator of $I = E_{\pi}[f]$ using M samples, x_1, x_2, \dots, x_M , of the Markov chain generated by P .

Thus, larger off-diagonal elements yield a smaller asymptotic variance v , leading to a smaller statistical error.

According to this theorem, a modified Gibbs sampler called the Metropolized Gibbs sampler was proposed [7, 8]. In the standard Gibbs sampler [5, 6], or the heat bath algorithm, the next state is chosen with a probability proportional to its weight independently of the current state. In the Metropolized Gibbs sampler, one proposes a state with a probability proportional to its weight, excluding the current state [22]. The proposed state is then accepted or rejected by the Metropolis algorithm (filter). Here we can assume the normalization $\sum_i^n \pi_i = 1$ since the normalization factor does not matter to the MCMC update. The resulting transition probabilities are given by

$$P_{ij}^{\text{MG}} = \min \left(\frac{\pi_i}{1 - \pi_j}, \frac{\pi_j}{1 - \pi_i} \right) \quad \forall i \neq j, \quad (7)$$

where the states are ordered such that $\pi_1 \leq \pi_2 \leq \dots \leq \pi_n$, and n is the number of possible states. For example, as studied below, we set $n = q$ for the single spin update of the q -state Potts model. The diagonal elements are determined from Eq. (7) and the probability conservation $\sum_i P_{ij} = 1$. It then follows that $P^{\text{MG}} \geq P^{\text{G}}$, where P^{G} is the transition matrix of the Gibbs sampler. Therefore, the Metropolized Gibbs sampler is more efficient than the Gibbs sampler. Note that the Metropolized Gibbs sampler reduces to the Metropolis algorithm for $n = 2$.

Let us define the rejection process as the process in which the next state is the same as the current state. The rejection probability is thus given by the diagonal elements of the transition matrix. The above transition probabilities (7) always lead to $P_{11}^{\text{MG}} = 0$; the rejection probability for the smallest-weight state becomes zero, which is referred to as the Metropolization for this state.

Interestingly, we can iterate this Metropolization scheme for other states and set $P_{ii} = 0$ for $1 \leq i \leq n - 1$ [8, 23]. The resultant transition probabilities are given by

$$P_{ij}^{\text{IMG}} = \begin{cases} y_i & (i < j) \\ \frac{\pi_i}{\pi_j} y_j & (i > j) \\ 1 - \sum_{k=1}^{n-1} y_k & (i = j = n) \\ 0 & (i = j < n), \end{cases} \quad (8)$$

where $y_1 = \pi_1/(1 - \pi_1)$ and

$$y_j = \frac{1 - \sum_{k=1}^{j-1} y_k \pi_j}{1 - \sum_{k=1}^j \pi_k} \quad (1 < j < n), \quad (9)$$

which we call the iterative Metropolized Gibbs sampler. This iterative sampler is generally more efficient than the simple Metropolized Gibbs sampler: $P^{IMG} \geq P^{MG}$.

In the meantime, a rejection-minimization algorithm [9] was proposed using the geometric allocation approach, which we call the Suwa–Todo algorithm. This algorithm and related rejection-minimization approaches were tested for several physical models and shown to be more efficient than the Metropolis algorithm, the heat bath algorithm, and even the iterative Metropolized Gibbs sampler [9, 18]. The Suwa–Todo algorithm produces a nonreversible Markov chain, so Peskun’s theorem does not apply to it.

Questions here are how much the rejection probability influences the efficiency of the MCMC method and whether the rejection process plays a major role in determining the efficiency both for reversible and nonreversible samplers. The primary purpose of the present paper is to answer these questions.

III. REJECTION-CONTROLLING ONE-PARAMETER TRANSITION KERNEL

To study how the rejection process affects the efficiency of the MCMC method and provide a flexible optimization approach, we propose a one-parameter transition kernel that enables control of the rejection probability. Our approach is an extension of the geometric allocation approach to optimizing stochastic flows between the possible states [9, 24].

We first calculate the cumulative weight distribution:

$$F_i = \sum_{j=1}^i \pi_j \quad (1 \leq i \leq n) \quad (10)$$

and $F_0 = 0$. Here the order of the states is arbitrary. Let us consider the sequence of F_i , or the weight tower, as illustrated in Fig. 1 (a) for $n = 6$. We then consider shifting the tower in a certain amount, as in Fig. 1 (b). The shift is periodic; the weight shifted over the top of the tower is allocated to the lowest part of the tower.

Using this weight shift, we determine the transition probability from the overlap between the original and the shifted towers. It is convenient to define the stochastic flow from i to j : $v_{ij} = \pi_i p_{i \rightarrow j}$, where $p_{i \rightarrow j}$ is the transition probability from i to j . Let s denote the amount of the shift, $0 < s < F_n$. In our approach, we set the stochastic flow v_{ij} to the overlap between the ranges $[F_{j-1}, F_j]$ and $[F_{i-1} + s, F_i + s]$. For example, the flows are determined in the case for $i = 1, 2$ and 3 in Fig. 1(b). If $F_i + s > F_n$, we take into account an additional overlap between the ranges $[F_{j-1} + F_n, F_j + F_n]$ and

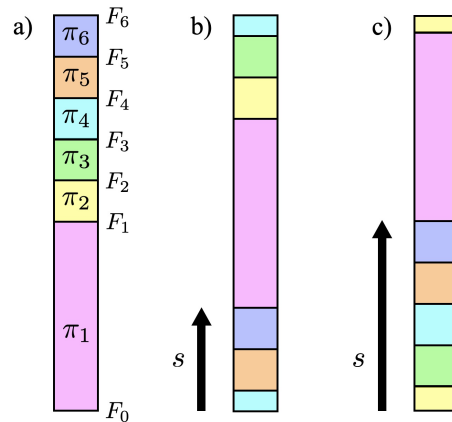


FIG. 1. (a) Example of the weight tower for $n = 6$ and (b) a periodic shift of the tower. π_i is the weight of state i , and F_i is the cumulative distribution. The stochastic flows and the transition probabilities are determined from the overlap between the original and the shifted towers for each state. See the main text for the details. (c) When $s = \max_i \pi_i$, this approach reduces to the Suwa–Todo algorithm [9].

$[F_{i-1} + s, F_i + s]$, assuming the tower to be periodic: e.g., for $i = 4, 5$ and 6 in Fig. 1(b). If a shifted weight range crosses the top of the original tower [Fig. 1(a)], nonzero flows are allocated from the overlaps in the above two cases, such as for $i = 4$ in Fig. 1(b) and $i = 2$ in Fig. 1(c). Because of the periodic shift, each range of π_i in the original tower is covered by the shifted tower. Therefore, this approach always satisfies the following condition:

$$\pi_i = \sum_j v_{ji} \quad \forall i, \quad (11)$$

equivalent to the global balance (1). We obtain the analytical expression of the stochastic flow determined by the periodic shift s :

$$v_{ij} = \max(0, \min(\Delta_{ij}, \pi_i + \pi_j - \Delta_{ij}, \pi_i, \pi_j)) + \max(0, \min(\Delta_{ij} - F_n, \pi_i + \pi_j + F_n - \Delta_{ij}, \pi_i, \pi_j)), \quad (12)$$

where

$$\Delta_{ij} = F_i - F_{j-1} + s, \quad (13)$$

which allows us to implement the present method easily. The transition probability is then set to $p_{i \rightarrow j} = v_{ij}/\pi_i$.

It is noteworthy that the present algorithm reduces to the Suwa–Todo algorithm [9] when we set $s = \max_i \pi_i =: \pi_{\max}$ depending on situations, as in Fig. 1(c). Thanks to the present extension to an arbitrary shift, it is straightforward to understand from the tower picture that a rejection-free solution, that is, $v_{ii} = \pi_i p_{i \rightarrow i} = 0 \forall i$, can be obtained for $\pi_{\max} \leq s \leq F_n - \pi_{\max}$ if $\pi_{\max} \leq F_n/2$, and no rejection-free solution exists otherwise. In particular, the choice of $s = F_n/2$ provides an optimal and reversible transition kernel with a minimized rejection

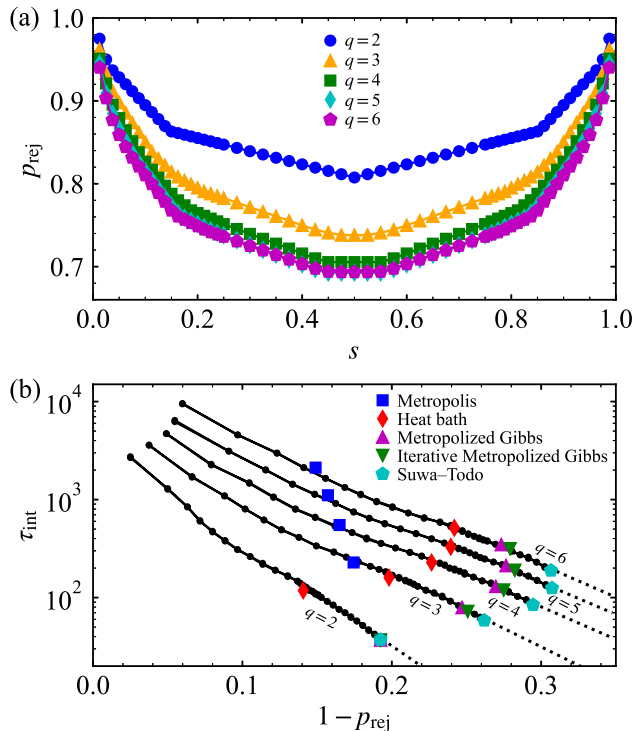


FIG. 2. (a) Rejection rate for each shift parameter s in the square lattice q -state Potts model for $L = 32$ and $q = 2, 3, 4, 5$ and 6 at the transition temperature. (b) Integrated autocorrelation time of the order parameter obtained using s (circles) plotted in (a) and several algorithms: the Metropolis algorithm (squares), the heat bath algorithm (diamonds), the Metropolized Gibbs sampler (upper triangles), the iterative Metropolized Gibbs sampler (lower triangles), and the Suwa-Todo algorithm (pentagons). The horizontal axis is $1 - p_{\text{rej}}$, where p_{rej} is the rejection rate measured during simulations. Each spin of the system is sequentially updated in a fixed order. The autocorrelation times in the compared algorithms almost fall on a single curve obtained using the present algorithm with different s . The dashed lines show fitted exponential functions: $\tau_{\text{int}} = ae^{-bp_{\text{rej}}}$, where a and b are the fitting parameters. The decay factor b is estimated to be 24 for $q = 2$, 17 for $q = 3$, and 15 for $q = 4, 5, 6$. The error bars are smaller than the symbol sizes.

probability. In contrast, the transition kernel is nonreversible for $s \neq F_n/2$. The present algorithm enables us to study the effect of the rejection probability by varying the shift parameter s .

In simulations, we calculate all the needed transition probabilities and prepare a look-up table of the probabilities before Monte Carlo sampling. We then use Walker’s alias method to generate a random event efficiently [25, 26], in which the computation time is $O(1)$ independent of the number of possible states n .

IV. RESULTS

We study how the rejection process affects the computation efficiency of the MCMC method using the q -state ferromagnetic Potts model [27]:

$$H = - \sum_{\langle ij \rangle} \delta_{\sigma_i, \sigma_j}, \quad (14)$$

where $\langle ij \rangle$ runs over all the pairs of nearest neighbor sites, $\sigma_i = 1, 2, \dots, q$ is the “spin” at site i , and δ is the Kronecker delta. This model shows the continuous phase transition for $q \leq 4$ and the first-order transition for $q > 4$ in the square lattice, while showing the continuous transition for $q = 2$ and the first-order transition for $q \geq 3$ in the simple cubic lattice. The transition temperature is analytically obtained in the square lattice model as $T_c = 1/\ln(1 + \sqrt{q})$ [27], while numerically estimated in the simple cubic lattice model to be $1/T_c = 0.44330910(6)$ [28], $0.550565(10)$ [29], and $0.628616(16)$ [30] for $q = 2, 3$ and 4 , respectively. Note that the $q = 2$ and 3 models are equivalent to the Ising and the three-state clock (\mathbb{Z}_3) models, respectively, and the $q = 4$ model is a special case of the Ashkin–Teller model [31, 32]. Experimental realizations of the Potts model have been proposed [33].

We calculate the order parameter defined by

$$O^2 = \frac{q-1}{q} \mathbf{m}^2, \quad (15)$$

where

$$\mathbf{m} = (m_1, m_2, \dots, m_q) \quad (16)$$

$$m_j = \frac{1}{N(q-1)} \left\langle \sum_k (q\delta_{j\sigma_k} - 1) \right\rangle, \quad (17)$$

N is the number of sites, and the bracket $\langle \cdot \rangle$ denotes the Monte Carlo average. To quantify the sampling efficiency of the Monte Carlo update, we calculated the integrated autocorrelation time (4) of the order parameter (15) at the transition temperature. We estimated the autocorrelation time from the asymptotic relation $\tau_{\text{int}} = \sigma^2/2\bar{\sigma}^2$, where σ^2 and $\bar{\sigma}^2$ are the mean squared error, or the square of the statistical error, calculated from the binning analysis and without binning [34]. For each Markov chain, we ran 2^{27} Monte Carlo steps, each consisting of N local spin updates, and discarded the first half for the thermalization (burn-in) process. We then calculated the integrated autocorrelation time and took the average over 128 independent Markov chains, which enables us to estimate the error bar reliably.

Varying the shift parameter introduced in Sec. III, we compare the autocorrelation time in the present algorithm and several reference algorithms: the Metropolis algorithm [4], the heat bath algorithm [5, 6], the Metropolized Gibbs sampler [7], the iterative

Metropolized Gibbs sampler [8], and the Suwa-Todo algorithm [9]. In the Metropolis algorithm, a state different from the current state was randomly proposed with probability $1/(n-1)$ and accepted/rejected by the standard Metropolis filter. In using the present algorithm, we fix the order of local spin states, which is equivalent to each other due to the permutation symmetry of the Potts model. We normalize the weight: $F_n = \sum_i^n \pi_i = 1$, so the shift parameter s can take $0 < s < 1$. Note that the Metropolized Gibbs samplers and the Suwa-Todo algorithm reduce to the Metropolis algorithm for $q = 2$.

Figure 2(a) shows the rejection rate measured during the simulations of the square lattice q -state Potts model at the transition temperature for each shift parameter s and $q = 2, 3, 4, 5$ and 6 . The system length was set to $L = 32$ and $N = L^2$. We here used the sequential spin update, in which the spins were swept sequentially in a fixed order. The rejection rate is symmetric to $s = 0.5$, as shown in Fig. 2(a). This symmetry is expected since the order of the local spin states is arbitrary in the Potts model, and the current choice is equivalent to the inverse order. Similar symmetric behavior of the transition rate is also expected for other models, e.g., the clock model [27].

Figure 2(b) shows the integrated autocorrelation time of the order parameter calculated using different s and the reference algorithms. Noticeably, the autocorrelation time decreases exponentially as the rejection rate is reduced. We fitted the autocorrelation time to an exponential function and obtained large decay factors, as shown in the caption. The decay factor is almost the same for $q = 4, 5$ and 6 , implying a universal property for $q \geq 4$ in two dimensions. Perhaps surprisingly, the autocorrelation times of the reference algorithms almost fall on a single curve obtained using the present algorithm with different s . This striking result indicates that the rejection process is essential to the Monte Carlo update, and the rejection probability almost determines the efficiency of the Monte Carlo sampling. The present algorithm with $s = 0.5$ ensures the detailed balance, while the Suwa-Todo algorithm does not. Nevertheless, the two algorithms produce almost the same autocorrelation time, suggesting that the stochastic flow created locally in the state space is insignificant. We likely need to use global state variables to induce effective stochastic flows, as the lifting technique considers [10–14]. We also calculated the integrated autocorrelation time of the total energy and found it shorter than that of the order parameter. The ratio of the two autocorrelation times is almost constant, independent of s . Thus, the present results are not specific to the order parameter but expected to be common among many quantities. Using a different system size only changes the prefactor of the autocorrelation time. Our main results do not depend on the system size.

To check whether the square lattice model is special, we calculate the rejection rate and the autocorrelation time in the simple cubic lattice model at the transition

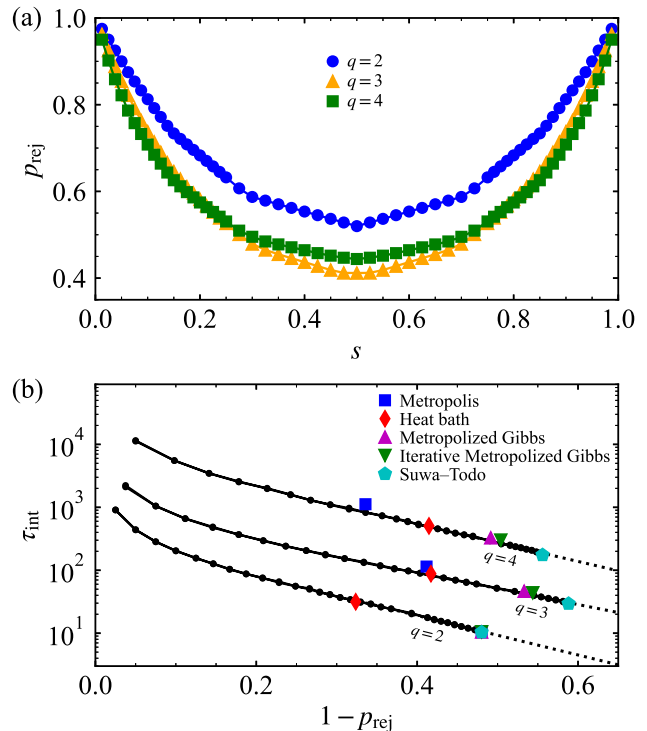


FIG. 3. (a) Rejection rate for each shift parameter s in the simple cubic lattice q -state Potts model for $L = 12$ and $q = 2, 3$ and 4 at the transition temperature. (b) Integrated autocorrelation time of the order parameter obtained using s (circles) plotted in (a) and several algorithms, as in Fig. 2. Although the Metropolis algorithm shows a slight deviation from the curve for $q = 3$ and 4 , the autocorrelation times in the reference algorithms are almost consistent with the curve obtained using the present algorithm with different s . The dashed lines show fitted exponential functions, and the decay factor is estimated to be 7.2 for $q = 2$, 5.9 for $q = 3$, and 6.9 for $q = 4$.

temperature for $q = 2, 3$ and 4 , as shown in Fig. 3. The system length was set to $L = 12$ and $N = L^3$. As the rejection probability is reduced, the autocorrelation time decreases exponentially, similarly to the case of the square lattice model. Although the Metropolis algorithm shows a slight deviation, the autocorrelation times in the reference algorithms almost collapse onto a single curve obtained using the present algorithm with different shift parameters, similarly to the case of the square lattice model. Therefore, the present exponential improvement is expected to be universal among various systems.

To study the update method dependence, we also test the random spin update, in which a spin (or a site) is randomly chosen for every update. Figure 4 shows the autocorrelation time in the square and cubic lattice models with $q = 4$ obtained using the random and the sequential spin updates. In contrast to the case of the sequential spin update, the autocorrelation time in the random spin update is well fitted to a power-law func-

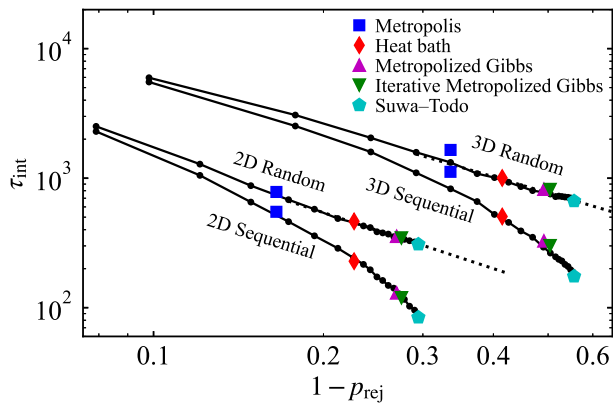


FIG. 4. Integrated autocorrelation time of the order parameter obtained using the random and sequential spin updates in the square (2D) and cubic (3D) lattice four-state Potts model at the transition temperature. The system sizes were set to $L = 32$ and 12 for the square and cubic lattice models, respectively. The dashed lines show fitted power-law functions for the random spin update: $\tau_{\text{int}} = \alpha(1 - p_{\text{rej}})^{-\gamma}$, where α and γ are the fitting parameters. The powers γ are estimated to be 1.4 and 1.3 for the 2D and 3D cases, respectively.

tion: $\tau_{\text{int}} \propto (1 - p_{\text{rej}})^{-\gamma}$. The estimated powers γ for the two- and three-dimensional models are noticeably close to each other, as shown in the caption of Fig. 4. Although the random spin update is more analytically tractable, the sequential spin update is superior to the random spin update as a sampling method. This fundamental difference between the rejection dependence of the sequential and the random spin updates highlights the nontrivial relation between the matrix elements and the eigenvalues of the transition matrix in the many-body system.

V. CONCLUSIONS

We have proposed a rejection-controlling one-parameter transition kernel for the MCMC method and

investigated the rejection effect on the sampling efficiency using the q -state ferromagnetic Potts model in the square and the simple cubic lattices. In the sequential spin update, the integrated autocorrelation time of the order parameter decreases exponentially as the rejection probability is reduced. The decay factor for $q = 4, 5$ and 6 is almost the same in two dimensions, implying a universal property of the system. In contrast, the autocorrelation time decreases algebraically in the random spin update. The significant difference between the rejection dependence of the sequential and the random spin updates emphasizes the nontrivial relation between the matrix elements and the eigenvalues of the transition matrix in the many-body system. Although the present and the reference algorithms construct considerably different transition matrix structures, the autocorrelation times of the compared algorithms almost fall on a single curve as a function of the rejection rate. Our finding indicates that the rejection probability is essential to the Monte Carlo update and almost determines the computation efficiency of an MCMC sampler. The present result establishes a straightforward guiding principle for the optimal transition kernel of discrete-variable interacting systems. Reducing the rejection probability is expected to produce efficient updates in various MCMC methods. Furthermore, it is possible for the present algorithm to optimize other quantities, such as net stochastic flows, in combination with the lifting technique [35]. It is of great interest to apply the present algorithm to other systems and generalize the argument to continuous variable systems in the near future.

ACKNOWLEDGMENTS

The author is grateful to Syngge Todo for the fruitful discussions. Simulations were performed using computational resources of the Supercomputer Center at the Institute for Solid State Physics, the University of Tokyo. This work was supported by the JSPS KAKENHI Grants-In-Aid for Scientific Research (No. 22K03508).

-
- [1] M.E.J. Newman and G.T. Barkema, *Monte Carlo Methods in Statistical Physics* (Oxford University Press, 1999).
 - [2] D. P. Landau and K. Binder, *A Guide to Monte Carlo Simulations in Statistical Physics*, 2nd ed. (Cambridge University Press, Cambridge, 2005).
 - [3] Christian P. Robert and George Casella, *Monte Carlo Statistical Methods*, 2nd ed. (Springer, New York, 2004).
 - [4] Nicholas Metropolis, Arianna W. Rosenbluth, Marshall N. Rosenbluth, Augusta H. Teller, and Edward Teller, "Equation of state calculations by fast computing machines," *The Journal of Chemical Physics* **21**, 1087–1092 (1953).
 - [5] Michael Creutz, "Monte carlo study of quantized su(2) gauge theory," *Phys. Rev. D* **21**, 2308–2315 (1980).
 - [6] Stuart Geman and Donald Geman, "Stochastic relaxation, gibbs distributions, and the bayesian restoration of images," *IEEE Transactions on Pattern Analysis and Machine Intelligence PAMI-6*, 721–741 (1984).
 - [7] Jun S. Liu, "Metropolized independent sampling with comparisons to rejection sampling and importance sampling," *Statistics and Computing* **6**, 113–119 (1996).
 - [8] Arnaldo Frigessi, Chii-Ruey Hwang, and Laurent Younes, "Optimal Spectral Structure of Reversible Stochastic Matrices, Monte Carlo Methods and the Simulation of Markov Random Fields," *The Annals of Applied*

- Probability* **2**, 610 – 628 (1992).
- [9] Hidemaro Suwa and Synge Todo, “Markov chain monte carlo method without detailed balance,” *Phys. Rev. Lett.* **105**, 120603 (2010).
- [10] Konstantin S. Turitsyn, Michael Chertkov, and Marija Vucelja, “Irreversible monte carlo algorithms for efficient sampling,” *Physica D: Nonlinear Phenomena* **240**, 410–414 (2011).
- [11] Heitor C.M. Fernandes and Martin Weigel, “Non-reversible monte carlo simulations of spin models,” *Computer Physics Communications* **182**, 1856–1859 (2011), computer Physics Communications Special Edition for Conference on Computational Physics Trondheim, Norway, June 23–26, 2010.
- [12] Raoul D. Schram and Gerard T. Barkema, “Monte carlo methods beyond detailed balance,” *Physica A: Statistical Mechanics and its Applications* **418**, 88–93 (2015), proceedings of the 13th International Summer School on Fundamental Problems in Statistical Physics.
- [13] Marija Vucelja, “Lifting—a nonreversible markov chain monte carlo algorithm,” *American Journal of Physics* **84**, 958–968 (2016).
- [14] Fahim Faizi, George Deligiannidis, and Edina Rosta, “Efficient irreversible monte carlo samplers,” *Journal of Chemical Theory and Computation* **16**, 2124–2138 (2020).
- [15] Etienne P. Bernard, Werner Krauth, and David B. Wilson, “Event-chain monte carlo algorithms for hard-sphere systems,” *Phys. Rev. E* **80**, 056704 (2009).
- [16] Manon Michel, Sebastian C. Kapfer, and Werner Krauth, “Generalized event-chain monte carlo: Constructing rejection-free global-balance algorithms from infinitesimal steps,” *The Journal of Chemical Physics* **140**, 054116 (2014).
- [17] P. H. Peskun, “Optimum Monte-Carlo sampling using Markov chains,” *Biometrika* **60**, 607–612 (1973).
- [18] Hidemaro Suwa and Synge Todo, “Geometric allocation approach for transition kernel of Markov chain,” in *Monte Carlo Methods and Applications: Proceedings of the 8th IMACS Seminar on Monte Carlo Methods* (2012) Chap. 23, pp. 213–221.
- [19] Hidemaro Suwa, “Geometric allocation approach to accelerating directed worm algorithm,” *Phys. Rev. E* **103**, 013308 (2021).
- [20] Ting-Li Chen, Wei-Kuo Chen, Chii-Ruey Hwang, and Hui-Ming Pai, “On the optimal transition matrix for markov chain monte carlo sampling,” *SIAM Journal on Control and Optimization* **50**, 2743–2762 (2012).
- [21] Hidemaro Suwa, *Geometrically Constructed Markov Chain Monte Carlo Study of Quantum Spin-phonon Complex Systems*, Springer Theses (Springer, 2014).
- [22] D. Loison, C. L. Qin, K. D. Schotte, and X. F. Jin, “Canonical local algorithms for spin systems: heat bath and hastings’s methods,” *The European Physical Journal B - Condensed Matter and Complex Systems* **41**, 395–412 (2004).
- [23] Lode Pollet, Stefan M. A. Rombouts, Kris Van Houcke, and Kris Heyde, “Optimal monte carlo updating,” *Phys. Rev. E* **70**, 056705 (2004).
- [24] S. Todo and H. Suwa, “Geometric allocation approaches in markov chain monte carlo,” *Journal of Physics: Conference Series* **473**, 012013 (2013).
- [25] Kouki Fukui and Synge Todo, “Order-n cluster monte carlo method for spin systems with long-range interactions,” *Journal of Computational Physics* **228**, 2629–2642 (2009).
- [26] Toshiaki Horita, Hidemaro Suwa, and Synge Todo, “Upper and lower critical decay exponents of ising ferromagnets with long-range interaction,” *Phys. Rev. E* **95**, 012143 (2017).
- [27] F. Y. Wu, “The potts model,” *Rev. Mod. Phys.* **54**, 235–268 (1982).
- [28] Youjin Deng and Henk W. J. Blöte, “Simultaneous analysis of several models in the three-dimensional ising universality class,” *Phys. Rev. E* **68**, 036125 (2003).
- [29] Wolfhard Janke and Ramon Villanova, “Three-dimensional 3-state potts model revisited with new techniques,” *Nuclear Physics B* **489**, 679–696 (1997).
- [30] Peter Arnold and Yan Zhang, “Monte carlo study of very weakly first-order transitions in the three-dimensional ashkin-teller model,” *Nuclear Physics B* **501**, 803–837 (1997).
- [31] J. Ashkin and E. Teller, “Statistics of two-dimensional lattices with four components,” *Phys. Rev.* **64**, 178–184 (1943).
- [32] Rodney J. Baxter, *Exactly Solved Models in Statistical Mechanics* (ACADEMIC PRESS, San Diego, 1982).
- [33] E Domany, Y Shnidman, and D Mukamel, “Type i FCC antiferromagnets in a magnetic field: a realisation of the q=3- and q=4-state potts models,” *Journal of Physics C: Solid State Physics* **15**, L495–L500 (1982).
- [34] Bernd A. Berg, *Markov Chain Monte Carlo Simulations and Their Statistical Analysis: With Web-based Fortran Code* (World Scientific Publishing, 2004).
- [35] Hidemaro Suwa, “Lifted directed-worm algorithm,” [arXiv , 2206.13881](https://arxiv.org/abs/2206.13881).